

SSC EMISSION AS THE ORIGIN OF THE GAMMA RAY AFTERGLOW OBSERVED IN GRB 980923

N. Fraija, M. M. González and W. H. Lee

Instituto de Astronomía, Universidad Nacional Autónoma de México, Apdo. Postal 70-264,
Cd. Universitaria, México DF 04510

nifraija@astro.unam.mx, mgonzalez@astro.unam.mx, wlee@astro.unam.mx

Received _____; accepted _____

ABSTRACT

GRB 980923 was one of the brightest bursts observed by the Burst and Transient Source Experiment (BATSE). Previous studies have detected two distinct components in addition to the main prompt episode, which is well described by a Band function. The first of these is a tail with a duration of $\simeq 400$ s, while the second is a high-energy component lasting $\simeq 2$ s. We summarize the observations, and argue for a unified model in which the tail can be understood as the early γ -ray afterglow from forward shock synchrotron emission, while the high-energy component arises from synchrotron self-Compton (SSC) from the reverse shock. Consistency between the main assumption of thick shell emission and agreement between the observed and computed values for fluxes, break energies, starting times and spectral indices leads to a requirement that the ejecta be highly magnetized.

Subject headings: gamma rays: bursts — radiation mechanisms: nonthermal

1. Introduction

The most successful theory in terms of explaining GRBs and their afterglows is the fireball model (see Mészáros 2006; Zhang & Mészáros 2004, for recent reviews). This model predicts an expanding ultrarelativistic shell that moves into the external surrounding medium. The collision of the expanding shell with another shell (internal shocks) or the interstellar medium (external shocks) gives rise to radiation emission through the synchrotron and SSC processes. In addition, when the expanding relativistic shell encounters the external medium two shocks are involved: an outgoing, or forward, shock (Rees & Mészáros 1994; Paczyński & Rhoads 1993) and another one that propagates back into the ejecta, the reverse shock (Mészáros & Rees 1994, 1997a).

According to the standard relativistic fireball model, the forward shock accelerates electrons (through first order Fermi mechanism or electric fields associated with the Weibel instability) up to relativistic energies and generates magnetic fields (Medvedev & Loeb 1999). The afterglow emission is more likely to be synchrotron (Sari et al. 1998); however inverse Compton scattering may affect the electron radiative cooling. The progressive, power-law deceleration of the forward shock leads to a continuous softening of the afterglow spectrum (Panaitescu 2007). This has been observed in the spectra and light curves of GRB 970228 (Sari et al. 1998), GRB 970508 (Panaitescu et al. 1998; Sari et al. 1998), GRB 980923 (Giblin et al. 1999) and among a dozen other afterglows (Zeh et al. 2006).

On the other hand, the reverse shock is predicted to produce a strong optical flash (Mészáros & Rees 1997a; Sari & Piran 1999a,b). When it crosses the shell, the reverse shock heats it up and accelerates electrons, but it operates only once. Thus, unlike the forward shock emission that continues later at lower energy, the reverse shock emits a single burst. After the peak of the reverse shock no new electrons are injected and the shell material cools adiabatically (Vedrenne & Atteia 2009). However, this picture can be modified allowing a long-lived reverse shock if the central engine emits slowly moving material in which the reverse shock

could propagate and survive for hours to days (Genet et al. 2007; Uhm & Beloborodov 2007). Now, although the contribution of the reverse shock synchrotron emission to the X-ray band is small, electrons in the reverse shock region can upscatter the synchrotron photons (SSC process) up to the X-ray band or even higher energies (Mészáros & Rees 1993; Wang et al. 2001a,b, 2005; Granot & Guetta 2003; Kobayashi et al. 2007a; Zhang et al. 2006).

The soft tail component seen in GRB980923 has been described reasonably well by synchrotron emission from a decelerating relativistic shell that collides with an external medium (forward shock model), and also described as such in more than a dozen independent events (see, e.g. Chevalier & Li 1999; Rhoads 1999; Sari et al. 1998; Panaitescu 2007; Giblin et al. 1999; Shao & Dai et al. 2005). The high energy component, on the other hand, has been explored through inverse Compton emission models (Granot & Guetta 2003; Pe’er & Waxman 2004) and SSC emission from the reverse shock (Wang et al. 2005; Kobayashi et al. 2007a; Wang et al. 2001b). In all cases a full description of the high energy component features has not been achieved.

In this paper we present a unified description of the tail and the high energy component in GRB980923 through a forward and reverse shock, accounting for their energy, spectral indices, fluxes and duration. In order to do so consistently we find that a magnetized outflow is required.

2. GRB 980923

GRB 980923 was observed by the Burst and Transient Source Experiment (BATSE) on 1998 September 23 at 20:10:52 UT for 32.02 s. It was localized to 234° with respect to the pointing-axis direction of CGRO. In agreement with the lightcurve given by González

et al. (2009, 2011) (Figure 1), the event consists of three components. The first is related to the typical prompt emission, the second one to a smooth tail which lasts ~ 400 s and the last to a hard component extending up to ~ 150 MeV. The smooth tail was well described by Giblin et al. (1999) as the evolution of a synchrotron cooling break in the slow-cooling regime starting at $t_0 = 32$ seconds. This conclusion was based on two different aspects. First, the time-dependent break energy was modeled with a power law of the form $E_0(t - t_0)^\delta$ and for $t_0 = 32.109$ seconds, they obtained $\delta = -0.52 \pm 0.12$. Second, in agreement with the computed value from the spectral index $p = 2.4 \pm 0.11$ and the value of t_0 , they obtained the relationship between the temporal and spectral indices and observed that the index values were indeed closer to the slow cooling regime. Thus, Giblin et al. (1999) identified the evolution of the spectrum in the tail of the burst as the evolution of a synchrotron cooling break in the slow-cooling regime, implying also that the transition from fast to slow cooling could take place on short timescales, comparable to the duration of the burst. On the other hand, González et al. (2009, 2011) described the high energy component peaking at $t = 20$ s as a power law with spectral index, γ of 1.439 ± 0.0687 and flux $F = 49.2 \pm 3.8$ erg cm² s⁻¹ and also pointed out that the tail could begin before or at least about 14s after the burst trigger. We assume González et al. (2009, 2011) results to develop a unified model where both components are related.

3. Dynamics of the forward and reverse shock

In this section, we first extend the work done by Giblin et al. (1999) on the smooth tail, and then proceed to compute the energy range for SSC emission from a thick shell of the reverse shock fireball to account for the hard component. We point out that the tail could have begun before or at least about 14s after the burst trigger, suggesting that before this time there already existed forward and reverse shocks, and find that the

characteristics of the observed hard emission noted by González et al. (2009, 2011) can be accounted for consistently by a scenario where the reverse shock becomes relativistic during its propagation, with magnetization parameter close to unity. The subscripts f and r refer throughout to the forward and reverse shock, respectively.

3.1. Choice of t_0

In general $t = 0$ is defined by the trigger time of the burst. Because of the connection between the very early afterglow (smooth tail) and this prompt emission, we plotted the power index δ as function of t_0 (Fig. 2) for the data and the power law of the form $E_0(t - t_0)^\delta$ (Giblin et al. 1999). It is clear that δ goes from fast cooling regime to slow cooling regime depending on the choice of t_0 . Also, we observe as a particular case that for $t_0 = 32\text{s}$, $\delta \sim 0.52$ is obtained (i.e. slow cooling). However, González et al. (2009, 2011) points out that the tail could begin before or at least about 14s after the burst trigger. From Fig. 3 we observe that the data used to define t_0 and δ are not very restrictive, so values of $t_0 = 14\text{s}$ and $\delta \sim 0.9$ are consistent the data too. Hence, choosing $t_0 = 14\text{s}$ gives a δ value in the transition from fast to slow cooling that can be explain if the transition time is sufficient short so that the spectra would be never observe in the fast cooling regime (this is the case we calculate later). we can assume that about this time the GRB ejecta collides with the ISM generating forward and reverse shocks.

3.2. Smooth tail from Synchrotron radiation forward shock

For the forward shock, we assume that electrons are accelerated in the shock to a power law distribution of Lorentz factor γ_e with a minimum Lorentz factor γ_m : $N(\gamma_e)d\gamma_e \propto \gamma_e^{-p}d\gamma_e$, $\gamma_e \geq \gamma_m$ and that constant fractions $\epsilon_{e,f}$ and $\epsilon_{B,f}$ of the shock energy go into the electrons

and the magnetic field, respectively. Then

$$\begin{aligned}\gamma_{m,f} &= \epsilon_{e,f} \left(\frac{p-2}{p-1} \right) \frac{m_p}{m_e} \gamma_f \\ &= 524.6 \epsilon_{e,f} \gamma_f\end{aligned}\tag{1}$$

where we have used the value of $p = 2.4 \pm 0.11$ as obtained by Giblin et al. (1999). Adopting the notation of (Sari et al. 1998) and ignoring self-absorption, the observed spectral flux in the fast-cooling regime is given by

$$F_\nu = F_{\nu,\max} \begin{cases} (\nu/\nu_{c,f})^{1/3}, & \nu_{c,f} > \nu \\ (\nu/\nu_{c,f})^{-1/2}, & \nu_{c,f} < \nu < \nu_{m,f}, \\ (\nu_{m,f}/\nu_{c,f})^{-1/2} (\nu/\nu_{m,f})^{-p/2}, & \nu > \nu_{m,f}. \end{cases}\tag{2}$$

Similarly, the flux in the slow-cooling regime can be written as

$$F_\nu = F_{\nu,\max} \begin{cases} (\nu/\nu_{m,f})^{1/3}, & \nu_{m,f} > \nu \\ (\nu/\nu_{m,f})^{-(p-1)/2}, & \nu_{m,f} < \nu < \nu_{c,f}, \\ (\nu_{c,f}/\nu_{m,f})^{-(p-1)/2} (\nu/\nu_{c,f})^{-p/2}, & \nu > \nu_{c,f}. \end{cases}\tag{3}$$

Using the typical parameters given by Björnsson (2001), we compute the typical and cooling frequencies of the forward shock synchrotron emission (Sari et al. 1998) which are given by,

$$\begin{aligned}\nu_{m,f} &\sim 1.9 \times 10^{19} \left(\frac{1+z}{2} \right)^{1/2} \left(\frac{\epsilon_{e,f}}{0.95} \right)^2 \epsilon_{B,f,-5}^{1/2} E_{54}^{1/2} t_1^{-3/2} \text{ Hz} \\ \nu_{c,f} &\sim 3.0 \times 10^{19} \left(\frac{1+z}{2} \right)^{-1/2} \left(\frac{1+x_f}{2.5} \right)^{-2} \epsilon_{B,f,-5}^{-3/2} n_{f,0}^{-1} E_{54}^{-1/2} t_1^{-1/2} \text{ Hz} \\ F_{\max,f} &\sim 2.2 \times 10 \left(\frac{1+z}{2} \right) \epsilon_{B,f,-5}^{1/2} n_{f,0}^{1/2} D_{28}^{-2} E_{54} \mu\text{Jy} \\ t_{\text{tr},f} &\sim 8.7 \left(\frac{1+z}{2} \right) \left(\frac{\epsilon_{e,f}}{0.95} \right)^2 \epsilon_{B,f,-5}^2 n_{f,0} E_{54} \text{ s}\end{aligned}\tag{4}$$

where the convention $Q_x = Q/10^x$ has been adopted in cgs units throughout this document unless otherwise specified. $t_{\text{tr},f}$ is the transition time, when the spectrum changes from fast

cooling to slow cooling, D is the luminosity distance, n_f is the ISM density, t is the time of the evolution of the tail, E is the energy, and the term $(1 + x_f)$ was introduced because a once-scattered synchrotron photon generally has energy larger than the electron mass in the rest frame of the second-scattering electrons. Multiple scattering of synchrotron photons can be ignored. x_f is given by (Sari et al. 2001) as:

$$x_f = \begin{cases} \frac{\eta \epsilon_{e,f}}{\epsilon_{B,f}}, & \text{if } \frac{\eta \epsilon_{e,f}}{\epsilon_{B,f}} \ll 1, \\ \left(\frac{\eta \epsilon_{e,f}}{\epsilon_{B,f}} \right)^{1/2}, & \text{if } \frac{\eta \epsilon_{e,f}}{\epsilon_{B,f}} \gg 1. \end{cases} \quad (5)$$

where $\eta = (\gamma_{c,f}/\gamma_{m,f})^{2-p}$ for slow cooling and $\eta = 1$ for fast cooling.

From eq. 4, we observe directly that $\nu_{m,f} \leq \nu_{c,f}$, the break energy $E_{c,f} \sim 124.1$ keV is consistent with the values given by (Giblin et al. 1999) and $t_{tr,f} \sim 8.7$ s, implying also that the transition from fast to slow cooling could take place on very short timescales, comparable to the duration of the burst, as expected

3.3. X ray flare from thick shell Reverse shock

For the reverse shock, it is possible to obtain a simple analytic solution in two limiting cases, thin and thick shell, (Sari et al. 1995) by using a critical Lorentz factor Γ_c ,

$$\begin{aligned} \Gamma_c &= \left(\frac{3E}{4\pi n_r m_p c^5 T^3} \right)^{1/8} \left(\frac{1+z}{2} \right)^{3/8} \\ &= 255.2 \left(\frac{1+z}{2} \right)^{3/8} n_{r,1}^{-1/8} E_{54}^{1/8} \left(\frac{T_{90}}{32s} \right)^{-3/8} \end{aligned} \quad (6)$$

where T_{90} is the time of the GRB, which is much larger than the peak time of the reverse shock emission, and n_r is the thick shell density. We consider the thick shell case in which the reverse shock becomes relativistic during the propagation and the shell is significantly decelerated by the reverse shock. Hence, the Lorentz factor at the shock crossing time t_c

is given by $\gamma_d \sim \Gamma_c$ (Kobayashi et al. 2007a; Kobayashi & Zhang 2007b), and for $\sigma \sim 1$, where $\sigma = L_{pf}/L_{kn} = B_r^2/4\pi n_r m_p c^2 \Gamma_r^2$ is the magnetization parameter, defined as the ratio of Poynting flux to matter energy flux, the crossing time t_c is much shorter than T_{90} , $t_c \sim T_{90}/6$, (Fan et al. 2004; Fan 2008; Zhang & Kobayashi 2005; Drenkhahn 2002). Now, if the constant fractions, $\epsilon_{e,r}$ and $\epsilon_{B,r}$ of the reverse shock energy go into the electrons and magnetic fields, respectively, we have

$$\begin{aligned} \gamma_{m,r} &= \epsilon_{e,r} \left(\frac{p-2}{p-1} \right) \frac{m_p \gamma_r}{m_e \Gamma_c} \\ &= 1233.5 \left(\frac{1+z}{2} \right)^{-3/8} \left(\frac{\epsilon_{e,r}}{0.6} \right) \gamma_{r,3} n_{r,1}^{1/8} E_{54}^{-1/8} \left(\frac{T_{90}}{32s} \right)^{3/8} \end{aligned} \quad (7)$$

where γ_r is the Lorentz factor of the thick shell. The spectral characteristics of the forward and reverse shock synchrotron emission are related (Zhang et al. 2003; Kobayashi et al. 2007a; Fan & Wei 2005; Fan et al. 2004; Jin & Fan 2007; Shao & Dai et al. 2005) by,

$$\begin{aligned} \nu_{m,r} &\sim \mathcal{R}_e^2 \mathcal{R}_B^{-1/2} \mathcal{R}_M^{-2} \nu_{m,f} \\ \nu_{c,r} &\sim \mathcal{R}_B^{3/2} \mathcal{R}_x^{-2} \nu_{c,f} \\ F_{\max,r} &\sim \mathcal{R}_B^{-1/2} \mathcal{R}_M F_{\max,f} \end{aligned} \quad (8)$$

where $\mathcal{R}_B = \epsilon_{B,f}/\epsilon_{B,r}$, $\mathcal{R}_e = \epsilon_{e,r}/\epsilon_{e,f}$, $\mathcal{R}_x = (1+x_f)/(1+x_r+x_r^2)$ and $\mathcal{R}_M = \Gamma_c^2/\gamma$. The previous relations tell us that including the re-scaling there is a unified description between both shocks (forward and reverse), and the distinction between forward and reverse magnetic fields considers that in some central engine models (Usov 1992; Mészáros & Rees 1997b; Wheeler et al. 2000) the fireball wind may be endowed with “primordial” magnetic fields. Also as the cooling Lorentz factor must be corrected, then \mathcal{R}_x is introduced as a correction factor for the IC cooling, where x_r is obtained by (Kobayashi et al. 2007a) as,

$$x_r = \begin{cases} \frac{\eta \epsilon_{e,r}}{\epsilon_{B,r}}, & \text{if } \frac{\eta \epsilon_{e,r}}{\epsilon_{B,r}} \ll 1, \\ \left(\frac{\eta \epsilon_{e,r}}{\epsilon_{B,r}} \right)^{1/3}, & \text{if } \frac{\eta \epsilon_{e,r}}{\epsilon_{B,r}} \gg 1. \end{cases} \quad (9)$$

For fast cooling , we take $\eta = 1$, and hence with the standard values for $\epsilon_{B,r}$ and $\epsilon_{e,r}$, $\eta\epsilon_{B,r}/\epsilon_{e,r} \sim 4.8$. Using equations (4) and (8), the typical and cooling frequencies of the reverse shock synchrotron emission are

$$\begin{aligned}\nu_{m,r} &\sim 3.4 \times 10^{16} \left(\frac{1+z}{2}\right)^{-1} \left(\frac{\epsilon_{e,r}}{0.6}\right)^2 \left(\frac{\epsilon_{B,r}}{0.125}\right)^{1/2} \gamma_{r,3}^2 n_{r,1}^{1/2} \text{ Hz}, \\ \nu_{c,r} &\sim 1.5 \times 10^{11} \left(\frac{1+z}{2}\right)^{3/2} \left(\frac{1+x_r+x_r^2}{6}\right)^{-2} \left(\frac{\epsilon_{B,r}}{0.125}\right)^{-7/2} n_{r,1}^{-3} E_{54}^{-1/2} \gamma_{r,3}^{-6} \left(\frac{T_{90}}{32s}\right)^{5/2} \text{ Hz}, \\ F_{\max,r} &\sim 5.02 \times 10^2 \left(\frac{1+z}{2}\right)^{7/4} \left(\frac{\epsilon_{B,r}}{0.125}\right)^{1/2} n_{r,1}^{1/4} D_{28}^{-2} E_{54}^{5/4} \gamma_{r,3}^{-1} \left(\frac{T_{90}}{32s}\right)^{-3/4} \text{ Jy}.\end{aligned}\quad (10)$$

From equation 10 we see that $\nu_{m,r}$ and $\nu_{c,r}$ correspond to optical and IR frequencies, respectively, and that $\nu_{m,r}$, which characterizes the frequency band, does not depend on x_r . However these energies were not recorded. Instead, as higher energy photons were observed we compute the upscattering emission of the synchrotron radiations (equations 2 and 3) ($r \rightarrow f$) by relativistic electrons (fast cooling and slow cooling (Sari et al. 2001)). So the SSC spectrum in the fast cooling regime is,

$$\nu F_\nu^{\text{SSC}} = (\nu F_\nu)_{\max}^{\text{SSC}} \begin{cases} (\nu_c^{\text{IC}}/\nu_m^{\text{IC}})^{1/2} (\nu/\nu_c^{\text{IC}})^{4/3} & \nu < \nu_c^{\text{IC}} \\ (\nu/\nu_m^{\text{IC}})^{1/2} & \nu_c^{\text{IC}} < \nu < \nu_m^{\text{IC}} \\ (\nu/\nu_m^{\text{IC}})^{(2-p)/2} & \nu > \nu_m^{\text{IC}} \end{cases} \quad (11)$$

and in the slow cooling regime we find

$$\nu F_\nu^{\text{SSC}} = (\nu F_\nu)_{\max}^{\text{IC}} \begin{cases} (\nu_m^{\text{IC}}/\nu_c^{\text{IC}})^{(3-p)/2} (\nu/\nu_m^{\text{IC}})^{4/3} & \nu < \nu_m^{\text{IC}} \\ (\nu/\nu_c^{\text{IC}})^{(3-p)/2} & \nu_m^{\text{IC}} < \nu < \nu_c^{\text{IC}} \\ (\nu/\nu_c^{\text{IC}})^{(2-p)/2} & \nu > \nu_c^{\text{IC}} \end{cases} \quad (12)$$

$\nu^{\text{(IC)}}$, $\nu_c^{\text{(IC)}}$ and $F_{\max}^{\text{(IC)}}$ are given by

$$\nu_m^{\text{(IC)}} \sim \gamma_m^2 \nu_{m,r}; \quad \nu_c^{\text{(IC)}} \sim \gamma_c^2 \nu_{c,r}; \quad F_{\max}^{\text{(IC)}} \sim k\tau F_{\max,r}; \quad (13)$$

where $k = 4(p - 1)/(p - 2)$ and $\tau = \frac{\sigma_T N_e}{4\pi R_d} = \frac{c}{3} \left(\frac{1+z}{2}\right)^{-1} \sigma_T n \Gamma_c^4 \gamma^{-1}$ is the optical depth of the shell. In agreement with equations (10) and (13), in the Self-Synchrotron Compton we have,

$$\begin{aligned}
 \nu_m^{(IC)} &\sim 1.034 \times 10^{23} \left(\frac{1+z}{2}\right)^{-7/4} \left(\frac{\epsilon_{e,r}}{0.6}\right)^4 \left(\frac{\epsilon_{B,r}}{0.125}\right)^{1/2} \gamma_{r,3}^4 n_{r,1}^{3/4} E_{54}^{-1/4} \left(\frac{T_{90}}{32s}\right)^{3/4} \text{ Hz}, \\
 \nu_c^{(IC)} &\sim 1.1 \times 10^{10} \left(\frac{1+z}{2}\right)^{3/2} \left(\frac{1+x+x^2}{6}\right)^{-4} \left(\frac{\epsilon_{B,r}}{0.125}\right)^{-7/2} n_{r,1}^{-3} E_{54}^{-1/2} \gamma_{r,3}^{-6} \left(\frac{T_{90}}{32s}\right)^{-5/2} \text{ Hz}, \\
 F_{\max}^{(IC)} &\sim 4.7 \times 10^{-2} \left(\frac{1+z}{2}\right)^{9/4} \left(\frac{\epsilon_{B,r}}{0.125}\right)^{1/2} n_{r,1}^{3/4} D_{28}^{-2} E_{54}^{7/4} \gamma_{r,3}^{-2} \left(\frac{T_{90}}{32s}\right)^{-5/4} \text{ Jy}. \tag{14}
 \end{aligned}$$

From equation 14 we observe that the break energies and $(\nu F)_{\max} = 21.2 \times 10^{-6} \text{ erg cm}^{-2} \text{ s}^{-1}$ are within the range pointed out by González et al. (2009, 2011).

4. Discussion and Conclusions

As shown in Figure 2, the power law decay index is sensitive to the chosen value of t_0 , so depending on our choice, we will be apparently closer to a fast or slow cooling regime. Choosing $t_0 \leq 14\text{s}$ (González et al. 2009, 2011; Sacahui et al. 2011a), and assuming that from this time until $t \sim 32\text{s}$ the synchrotron emission was eclipsed by the prompt phase, we have calculated the transition time from fast to slow cooling as $\sim 8.7\text{s}$. Thus, 18s later, at $t = 32\text{s}$ the synchrotron process generated by the forward shock was in the slow-cooling regime and in the energy range corresponding to that reported by Giblin et al. (1999). Also, we suggest that the diminishing flux at $\simeq 14\text{ s}$ may be due to pair production ($\gamma\gamma \rightarrow e^+e^-$) between prompt emission and forward shock photons (equation 4) at the beginning of the afterglow. We have calculated the energy of the forward shock photons as 1.31 MeV and the time for this energy to decrease under the pair production umbral as 1.5s which is consistent with duration of the diminishing flux.

In the reverse shock, the synchrotron process emitted photons with $\nu_{c,r} \sim 1.0 \times 10^{10}$ Hz and $\nu_{m,r} \sim 4.6 \times 10^{16}$ Hz, which were not recorded but were upscattered by electrons up to break energies $E_c^{IC} \sim 4.2 \times 10^{-5}$ eV, $E_m^{IC} \sim 427.9$ MeV with a $(\nu F)_{\max} = 21.2 \times 10^{-6}$ erg cm $^{-2}$ s $^{-1}$, which were pointed out by González et al. (2009, 2011) and Sacahui et al. (2011a). Now, in accordance with the observed value for the spectral index $\gamma \sim 1.44 \pm 0.07$, $\nu_{m,r}^{(ic)} > \nu_{c,r}^{(ic)}$ we conclude the SSC spectrum corresponds to fast-cooling regime, very similar to GRB 941017 (González et al. 2003; Granot & Guetta 2003). For our case (thick case), the flare occurs during the prompt gamma-ray phase.

From the value of \mathcal{R}_B , we obtained that the forward and reverse magnetic fields are related by $B_f = 0.9 \times 10^{-3} B_r$. The previous result indicates that there is a stronger magnetic field in the reverse-shock region than in the forward shock region, which may suggest that the obtained results are given when the ejecta is highly magnetized, as in the interpretation of the early afterglow of GRB 990123 and GRB 021211 provided by Zhang et al. (2003).

Finally, because the Large Area Telescope (LAT) covers the energy range from about 20 MeV to more than 300 GeV, we hope to detect other hard components in GRBs and so further constrain this model.

The current model accounts for the main characteristics of the burst: energies, spectral indices, fluxes, duration of the main components in a unified manner. The main requirements are that the ejecta be magnetized, leading to the formation of a reverse shock. The model has eight free parameters (equipartition magnetic field, equipartition electron energy, Lorentz factor, and densities all of the in the reverse and forward shocks), with standard values. The main difference between our model and previous models (Wang et al. 2005; Kobayashi et al. 2007a; Wang et al. 2001b) are the assumption of different equipartition values in the forward and reverse shock which leads the magnetization of the jet.

This burst has similar characteristics to GRB 090926A (Ackermann et al. 2011), but the high energy extended emission component may require SSC from the forward shock (Sacahui et al. 2011b).

We thank Enrico Ramírez-Ruiz and Charles Dermer for useful discussions. This work is partially supported by UNAM-DGAPA PAPIIT IN105211 (MG) and CONACyT 103520 (NF) and 83254 (WL).

REFERENCES

- Ackermann M., et al., 2011, ApJ, 729, 2
- Björnsson, C.-I. 2001, ApJ, 554, 593
- Chevalier R. & Li Z., 1999, ApJ, 520, L29
- Drenkhahn G., 2002, A&A, 387, 714
- Fan Y. Z., Wei, D.M. & Wang C.F., 2004, MNRAS, 351, L78
- Fan Y. Z. & Wei D.M., 2005, MNRAS, 364, L42
- Fan Y. Z., Wei D. M. & Wang C.F. , 2004, A&A, 424, 477
- Fan Y. Z. 2008, AIP conference Proceedings 1065, 159
- Genet, F., Daigne, F. & Leonard, P.J.T., 2007, MNRAS, 381, 372
- Giblin, T. W., et al. 1999, ApJ, 524, L47
- González M.M. et al. 2003, Nature, 424, 749.
- González M. M., Sacahui J. R. & Dignus B., 2009, AIP conference Proceedings 1133, 409
- González et al. 2011, ApJ, in preparation
- Granot, J. & Guetta, D. 2003, ApJ, 598, L11
- Jin, Z. P. & Fan Y.Z., 2007, MNRAS., 378, 1043
- Kobayashi, S., Zhang, B., Mészáros, P. & Burrows, D. 2007, ApJ, 655, 391
- Kobayashi, S. & Zhang, B. 2007, ApJ, 655, 973
- Medvedev M. & Loeb A., 1999, ApJ, 526, 697

- Mészáros, P. & Rees, M. J., 1993, *ApJ*, 418, L59
- Mészáros, P. & Rees, M. J., 1994, *MNRAS*, 269, L41
- Mészáros, P. & Rees, M. J., 1997a, *ApJ*, 476, 232
- Mészáros, P. & Rees, M. J., 1997b, *ApJ*, 482, L29
- Mészáros, P. 2006, *Report of Progress in Physics*, 69, 2259
- Paczynski B. & Rhoads J., 1993, *ApJ*, 418, L5
- Panaitescu A., Mészáros, P. & Rees, M. J., 1998, *ApJ*, 503, 314
- Panaitescu A. 2007, *MNRAS*, 379, 331
- Pe'er A & Waxman L, 2004, *ApJ*, 603, L1
- Rhoads J., 1999, *ApJ*, 525, 737
- Rees, M. J. & Mészáros, P., 1994, *ApJ*, 430, L93
- Sacahui J. R., González M. M., & Ramirez J. L., 2011, *RevMexAAsc* in Press.
- Sacahui J. R. et. al. in preparation.
- Sari, R., & Piran, T. 1995, *ApJ*, 455, L143
- Sari, R., Piran, T. & Narayan R. 1998, *ApJ*, 497, L17
- Sari, R., & Piran, T. 1999a, *A&AS*, 138, 537
- Sari, R., & Piran, T. 1999b, *ApJ*, 520, 641
- Sari R. & Esin A. A. 2001 *ApJ*, 548, 787
- Shao, L. & Dai, Z. G., 2005, *ApJ*, 633, 1027

- Uhm, Z. L., & Beloborodov A. M., 2007, ApJ, 665, L93
- Usov, V. V., 1992, Nature, 357, 472
- Vedrenne, G. & Atteia J.-L., 2009, Gamma-Ray Bursts: The brightest Explosions in the Universe, Springer, 276
- Wang, X. Y., Dai, Z. G. & Lu, T. 2001a, ApJ, 546, L33
- Wang, X. Y., Dai, Z. G. & Lu, T. 2001b, ApJ, 556, 1010
- Wang, X. Y., Cheng, K.S., Dai, Z. G. & Lu, T. 2005, A&A, 439, 957
- Wheeler, J. C., Yi. I., Höflich, P. & Wang, L. 2000, ApJ, 537, 810
- Zeh, A., Klose S. & Kann D. 2006 ApJ, 637, 889
- Zhang, B., Kobayashi, S. & Mészáros, P. 2003 ApJ, 595, 950
- Zhang, B. & Mészáros, P. 2004, Int. J. Mod. Phys., A19, 2385
- Zhang, B. et al. 2006 ApJ, 642, 354
- Zhang, B. & Kobayashi, S. 2005 ApJ, 628, 315

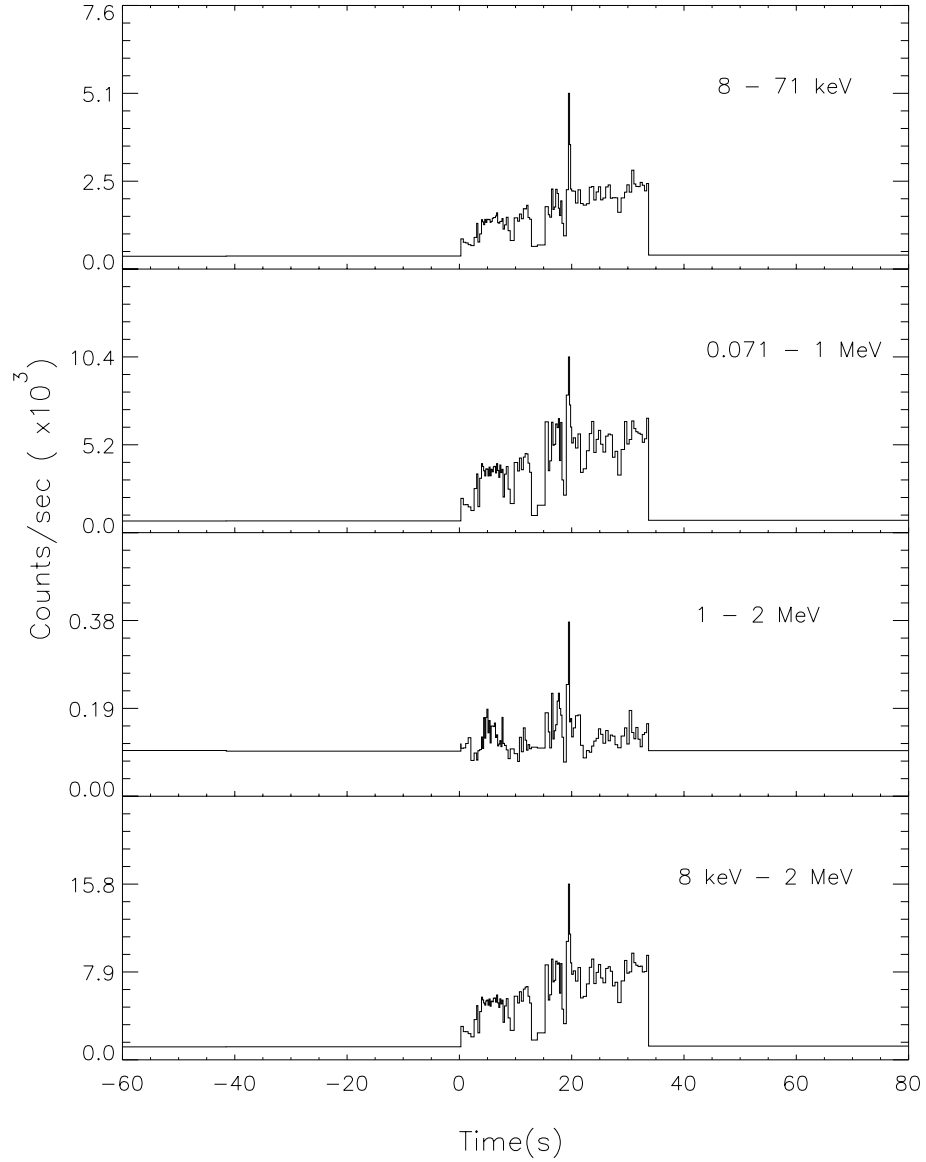


Fig. 1.— The BATSE SD7 count rates for GRB980923 are plotted in four energy ranges. A peak at 20 s is apparent, and stands out particularly at the low and high energy ranges.

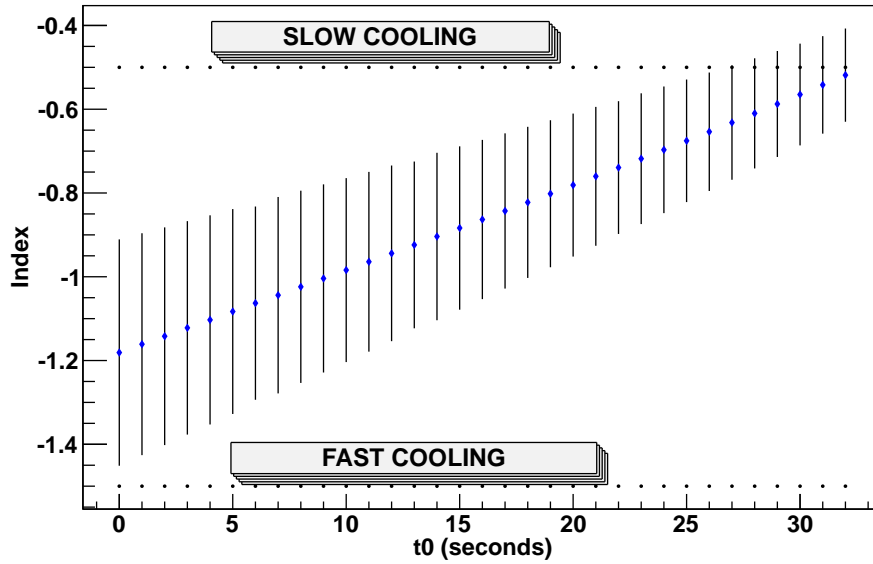


Fig. 2.— The power-law decay index δ is plotted as a function of t_0 for a power law of the form $E_0(t - t_0)^\delta$, where t_0 is the time at which the tail begins. The error bars are obtained for the different fits, as shown in figure 3. The index is sensitive to the value t_0 , and thus the choice of t_0 is crucial and illustrates the effect on the light-curves and therefore on the apparent evolution of the spectrum. The expected values for the slow and fast cooling regimes are indicated.

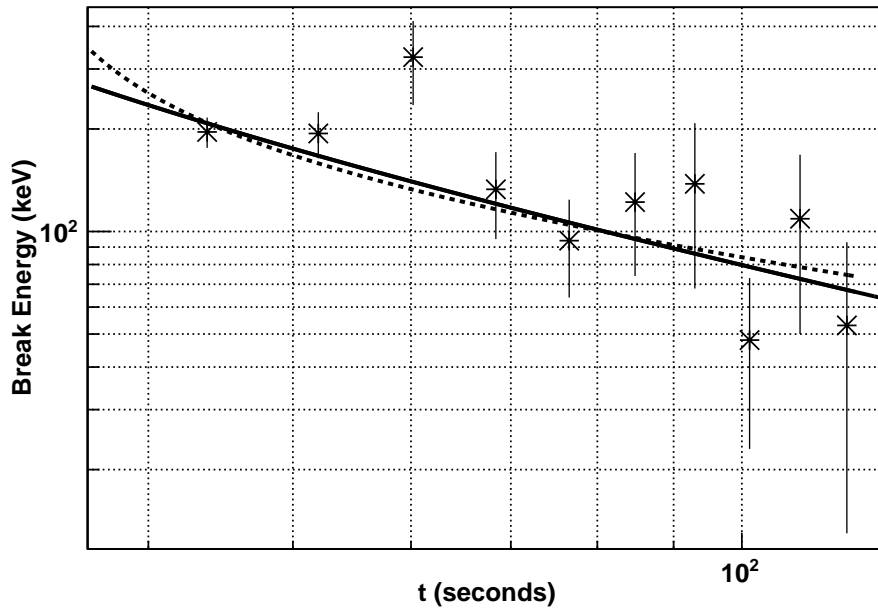


Fig. 3.— Break energy as a function of time t on logarithmic axes. The continuous line represents the fitted power law slope 0.5186 ± 0.1113 for $t_0 = 32$ s (Giblin et al. 1999), while the dashed line is the fitted power law slope 0.9039 ± 0.1999 for $t_0 = 14$ s. $t = 0$ corresponds to the burst trigger.